Molecular Aggregation Structure and Surface Properties of Poly(fluoroalkyl acrylate) Thin Films

Koji Honda,[†] Masamichi Morita,[†] Hideyuki Otsuka,[†,‡] and Atsushi Takahara[*,†,‡]

Department of Chemistry and Biochemistry, Graduate School of Engineering, Kyushu University, Hakozaki, Higashi-ku, Fukuoka 812-8581, Japan, and Institute for Materials Chemistry and Engineering, Kyushu University, Hakozaki, Higashi-ku, Fukuoka 812-8581, Japan

Received February 24, 2005; Revised Manuscript Received April 30, 2005

ABSTRACT: The effects of side chain length on the molecular aggregation states and surface properties of poly(fluoroalkyl acrylate) [PFA-C_y, where y is the fluoromethylene number of the R_f groups] thin films were systematically investigated. Spin-coated PFA-C_y thin films were characterized by static and dynamic contact angle measurements, X-ray photoelectron spectroscopy (XPS), differential scanning calorimetry, and wide-angle X-ray diffraction. The receding contact angles showed small values for PFA-C_y with short side chain ($y \leq 6$) and increased for ones with $y \geq 8$. It has been revealed that PFA-C_y with $y \geq 8$ was crystallized and formed ordered structures. These results suggest that the water-repellent mechanism of PFA-C_y can be attributed to the presence of highly ordered fluoroalkyl chains at the outermost surfaces. The results of XPS in the dried and hydrated states and the contact angle measurement in water indicate that the contact angle for water is lowered by exposure of the carbonyl groups to the water interface through reorientation of short fluoroalkyl chains.

Introduction

It has been well-known that polymers with fluoroalkyl (R_f) groups have surface characteristics that differ greatly from those of comparable hydrogenated structures: for example, excellent chemical and thermal stability, nonadhesive properties, low friction coefficients, low surface free energies,[1] and nonfouling behavior.[2] Most of them are poly(fluoroalkyl acrylate)s with long R_f groups, and these polymers have very low critical surface tension (γ_c), ranging from 8 to 11 mN m^{-1}.[3−5] These values are much lower than the 18 mN m^{-1} of polytetraflouoroethylene (PTFE), which is a typical fluoropolymer. The γ_c of closely packed $-CF_3$ groups (6 mN m^{-1}) is lower than that of the $-CF_2-$ surface (18 mN m^{-1}).[6] In poly(fluoroalkyl acrylate)s, the tighter the packing of the R_f groups, the greater the increase in density of the $-CF_3$ terminal groups. They therefore have a very low γ_c and have been used as surface modifiers for textiles and polymeric materials.[7]

The thermal stability and mechanical characteristics of poly(fluoroalkyl acrylate)s depend on the properties of the hydrocarbon of main chain, whereas the surface properties depend on the chemical structures of the R_f groups at the side chain. Surface reorientation of polar groups in contact with water has been investigated.[8−13] For example, it has been reported that poly(fluoroalkyl acrylate)s with short R_f groups have poor dynamic water repellency because of the high surface molecular mobility.[14] This phenomenon relates to the crystallinity of the R_f groups, and the crystallization of side chains is important for stable surface properties.[1] However, a detailed mechanism for this poor dynamic water repellency has not yet been clarified.

The authors have studied the surface properties and aggregation structure of side chains of fluoroalkyl acrylate polymer with the R_f groups and have attempted to establish guidelines for preparation of novel high-performance R_f polymers. In this paper, the authors discuss the relationship between surface properties and the chain length of the R_f groups of poly(fluoroalkyl acrylate)s [PFA-C_y, where y is the fluoromethylene number of the R_f groups] and clarify the water-repellent mechanism of PFA-C_y thin films.

Experimental Section

1. Materials. Polymerization. The chemical structure of PFA-C_y is shown in Chart 1. Fluoroalkyl acrylate monomers and 1,1,1,4,4,4-hexafluoro-2,2,3,3-tetrachlorobutane (CFC-316) were provided by Daikin Industries Co., Ltd. PFA-C_y were prepared by radical polymerization under a nitrogen atmosphere in 3,3-dichloro-1,1,1,2,2-pentafluoropropane (HCFC-225) at 323 K for 18 h for $y = 1$, 2, 4, 6, and 8 and in CFC-316 at 363 K for 18 h for $y = 10$, using azobis(isobutyronitrile) (AIBN) as an initiator.[15] The polymers, except for PFA-C_1, were purified by precipitation in methanol. PFA-C_1 was precipitated in hexane. PFA-C_1, -C_2, -C_4, and -C_6 were obtained as rubbery solids, and PFA-C_8 and -C_{10} were obtained as a white powder.

Preparation of Thin Polymer Films. PFA-C_y, except for PFA-C_{10}, was dissolved in HCFC-225 (concentration 1 wt %), and Si wafer was coated with solution by the spin-coating method (2000 rpm, 30 s). PFA-C_{10} was dissolved in CFC-316 (concentration 1 wt %) by heating at 373 K, and the Si wafer was coated with the solution at 373 K by the same method, as this polymer could not be dissolved in HCFC-225 and CFC-316 at room temperature. The film thickness was estimated as ≈100 nm by atomic force microscope measurement (AFM). The AFM observation was performed with an SPA 4000 (Seiko Instruments Inc.). AFM images were obtained under constant force mode in air at 300 K using a 100 μm × 100 μm scanner and a Si_3N_4 tip on a triangle cantilever with a spring constant of 0.032 N m^{-1}. The films were not annealed, unless it is mentioned otherwise.

2. Measurements. Wetting properties were evaluated by static and dynamic contact angle measurements. The crystalline states of PFA-C_y were determined by wide-angle X-ray diffraction (WAXD). Thermal analysis was carried out by differential scanning calorimetry (DSC). Surface reorganization of PFA-C_y thin film was evaluated by X-ray photoelectron spectroscopy (XPS) and the contact angle measurement in water.

[†] Graduate School of Engineering.
[‡] Institute for Materials Chemistry and Engineering.
* Corresponding author. E-mail takahara@cstf.kyushu-u.ac.jp.

10.1021/ma050394k CCC: $30.25
Published on Web 06/04/2005

Chart 1. Chemical Structure of Poly(perfluoroalkyl acrylate)s [PFA-C_y, Where y is the Fluoromethylene Number of the R_f Groups] ($x = 1$ for $y = 1$ and 2, $x = 2$ for $y = 4$, 6, 8, and 10)

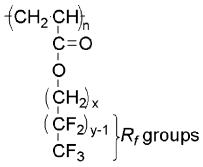

Contact Angle Measurement (in Air). The static and dynamic contact angles were measured on a DSA-10 (Krüss Co., Ltd.). The static contact angles of water and methylene iodide (each droplet volume was 2 μL) were measured, and the surface free energy was calculated from the static contact angles using Owens and Wendt's equation.[16] The dynamic contact angles were measured using an inclinable plane.[17] In an inclinable plane, a sample on a stage was tilted until a 50 μL water droplet began to slide down onto the sample. Subsequently, an advancing contact angle (θ_a), a receding contact angle (θ_r), and a sliding angle (θ_s) were determined.

DSC. The DSC data were obtained from a DSC8230 (Rigaku Denki Co., Ltd.). The heating rate was 10 K/min for a sample of 3 mg in an Al pan. Before the DSC measurements, the samples were preheated to 473 K to eliminate the effects of thermal history. Subsequently, the samples were cooled to 173 K and then measured from 173 to 473 K.

WAXD. The WAXD measurements were carried out on a Rigaku RINT 2500V (Rigaku Denki Co., Ltd.) with a Cu Kα X-ray source (40 kV, 200 mA) for powder and spin-coated thin films of PFA-C_y. The wavelength, λ, of the incident X-ray was 0.1542 nm. The data collection time was 3 s per step at 0.05° intervals. WAXD measurements were carried out by the symmetrical reflection geometry. In this method, Bragg diffraction from crystallographic planes parallel to the substrate is obtained from bulk regions.

XPS. The XPS measurements were carried out on a PHI5800 (Physical Electronics Co., Ltd.) with an Al Kα X-ray source. The X-ray gun was operated at 14 kV and 350 mW, and the analyzer chamber pressure was 10^{-9}–10^{-10} Pa. Takeoff angles were kept constant at 45°. The sample stage was cooled to ≈223 K during the measurement using liquid nitrogen to prevent the damage of fluorine atoms by X-ray exposure. The samples were measured in the hydrated state to characterize the suspected surface chemical composition in water.[8,11–13] In the hydrated state, the samples were hydrated by immersion in water ($T = 300$ K) for 120 min and then dried under vacuum (60 Pa) for 120 min, after which they were immediately measured. Using the surface in a dried state as a reference, we defined reorganization as a change from a hydrated surface composition to a dried one.

Contact Angle Measurement in Water. The static contact angles of methylene iodide and air bubbles on PFA-C_y films in water were measured by Hamilton's method[18,19] using DSA10. The sample was immersed in water ($T = 300$ K) for 120 min, and the contact angle was measured. The surface free energy in water was calculated from the static contact angles using the geometrical mean approach.[19]

Results and Discussion

Contact Angle Measurements (in Air). Figure 1 shows the dependence of (a) the static contact angle against water and methylene iodide, (b) the surface free energy, and (c) the dynamic contact angle against water on the fluoromethylene number of the R_f groups. The static contact angles and advancing contact angles (θ_a) were very high (above 100°), independent of the fluoromethylene number of the R_f groups. (When the fluoromethylene number was 1 or 2, the values were slightly lower.) On the other hand, the receding contact angle (θ_r) showed a small value for the PFA-C_y with

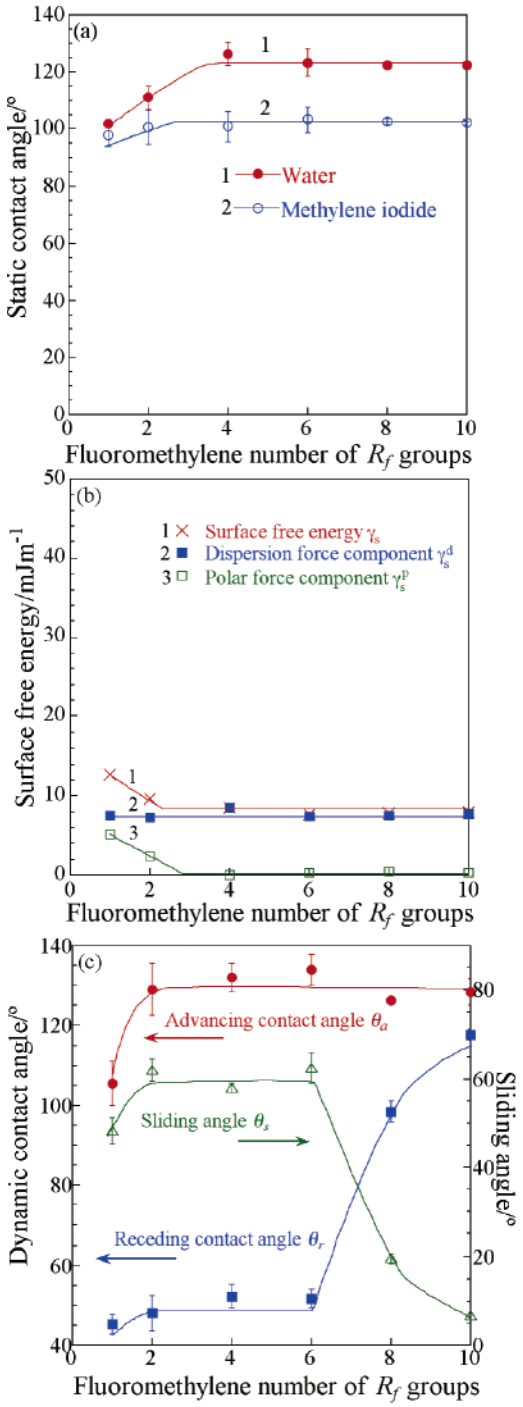

Figure 1. Dependence of (a) the static contact angles against water and methylene iodide (each droplet volume was 2 μL, $T = 292$ K), (b) the surface free energy, and (c) the dynamic contact angle and sliding angle against water (an inclinable plane, the droplet volume was 50 μL, $T = 292$ K) on the fluoromethylene number of the R_f groups.

$y \leq 6$ and increased drastically for $y \geq 8$. The contact angle hysteresis, $\Delta\theta$, which is expressed as $\theta_a - \theta_r$, with movement of the liquid front is often a result of surface roughness, heterogeneity, reorientation, and mobility.[5,20] The AFM observation of the film surface revealed the roughness is small enough not to give a large influence on the contact angle hysteresis.[21] Hence, in this case, the contribution of reorientation and mobility of side chain to $\Delta\theta$ is expected. This result therefore suggests that the surface reorientation occurred by exposure of

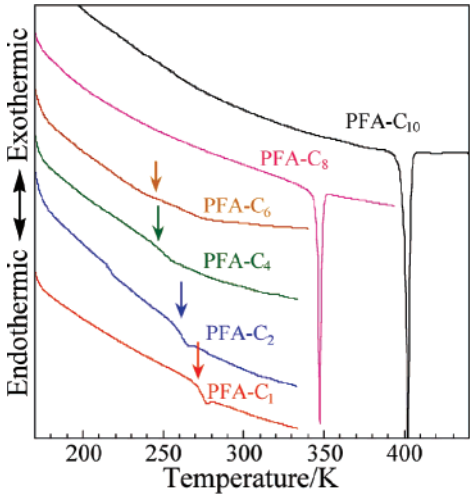

Figure 2. DSC thermograms of PFA-C_y ($y = 1$, 2, 4, 6, 8, and 10). The heating rate was 10 K/min.

the PFA-C_y ($y \leq 6$) surface to water. A similar result was reported for poly(alkyl methacrylate)s.[10] This phenomenon may be explained by an increased mobility of the R_f groups with $y \leq 6$.

PFA-C_y with $y \leq 6$ showed a higher sliding angle, θ_s, than PFA-C_y with $y \leq 6$, and θ_s decreased drastically for $y \geq 8$ as in θ_r. The relationship between the sliding angle and dynamic contact angle is given by eq 1[22−25]

$$mg(\sin \theta_s)/w = \gamma_l(\cos \theta_r - \cos \theta_a) \qquad (1)$$

where m, w, and γ_l are the mass of liquid droplet, the width of the droplet (orthogonal to the direction of drop movement), and the surface tension of liquid, respectively. The equation predicts the minimum angle of tilt (θ_s) at which a droplet will move spontaneously. It is clear from this equation that the hysteresis is an important factor for the sliding drops. The large contact angle hysteresis for PFA-C_y with $y \leq 6$ results in a very large sliding angles. On the other hand, the small contact angle hysteresis for PFA-C_y with $y \geq 8$ results in a very small sliding angle.

The following investigations were carried out in order to prove the above assumption.

Thermal Analysis. Figure 2 shows DSC thermograms of PFA-C_y. The melting temperature (T_m) of the side chain crystallites were clearly observed at 348 and 403 K for PFA-C_y with $y = 8$ and 10, respectively. In contrast, the glass transition temperature (T_g) were observed at 271, 259, 249, and 243 K for PFA-C_y with $y = 1$, 2, 4, and 6, respectively. The decrease in T_g with side chain length suggests that the extra free volume of the side chain acts as an internal plasticizer.[26] This behavior is similar to that observed for poly(alkyl methacrylate)s.[27] This internal plasticization affects the increase in the mobility of the R_f groups with $y \leq 6$, causing the surface reorientation. With an increase in the R_f side chain length, the R_f side chain becomes crystallizable due to the inter-side-chain interaction of the fluoroalkyl groups. Because the T_m of the R_f side chains are higher than the room temperature, stable surface hydrophobicity is expected for PFA-C_y with $y = 8$ and 10.

Molecular Aggregation States. Figure 3 shows powder WAXD profiles of PFA-C_y. PFA-C_y with $y \leq 6$ had no sharp peak. Diffraction peaks for PFA-C_y with $y \geq 8$ at $q = 1-9$ and 13 nm^{-1} were observed. Peaks at

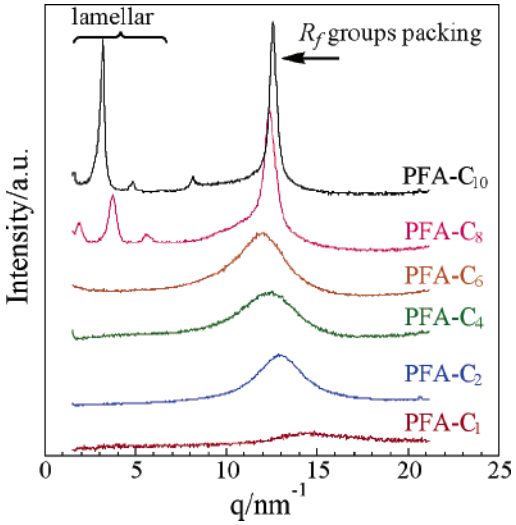

Figure 3. Powder WAXD profiles of PFA-C_y. The λ of incident X-ray was 0.1542 nm. The date collection time was 3 s per step, and the angular interval between step was 0.05°.

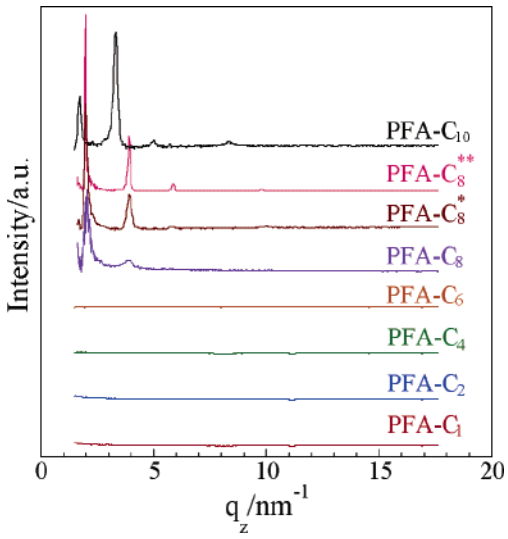

Figure 4. WAXD (symmetric reflection method) profiles of spin-coated PFA-C_y thin films (*annealed at 333 K for 6 h, **annealed at 348 K for 6 h). The λ of incident X-ray was 0.1542 nm. The data collection time was 3 s per step, and the angular interval between steps was 0.05°.

$q = 1-9$ nm^{-1} were assignable to the lamellar structure in which R_f groups are ordered like multilayer (the spacing $d = 3.4$ nm [PFA-C_8] and 3.9 nm [PFA-C_{10}], with these values being in agreement with the length of the two R_f groups),[28−30] and peaks at $q = 13$ nm^{-1} were assignable to the packing of R_f groups ($d = 0.50$ nm, which is close to the intermolecular distance of the PTFE crystal [$d = 0.49$ nm], which has the closest hexagonal packing of fluoroalkyl chains).[31,32] Thus, PFA-C_y with $y \leq 6$ are in a rubbery state and are expected to show high surface mobility at room temperature, while PFA-C_y with $y \geq 8$ are in the crystalline state and show low surface mobility.

Figure 4 shows WAXD (symmetric reflection method) profiles of spin-coated PFA-C_y thin films. Diffraction peaks assignable to the lamellar structure of R_f groups were observed in the cases of PFA-C_y with $y \geq 8$, similar to those in powder WAXD. However, the peak assignable to the hexagonal packing of R_f groups ($q = 13$ nm^{-1}) was not observed. In the symmetrical reflection method, Bragg diffraction from the crystallographic plane that

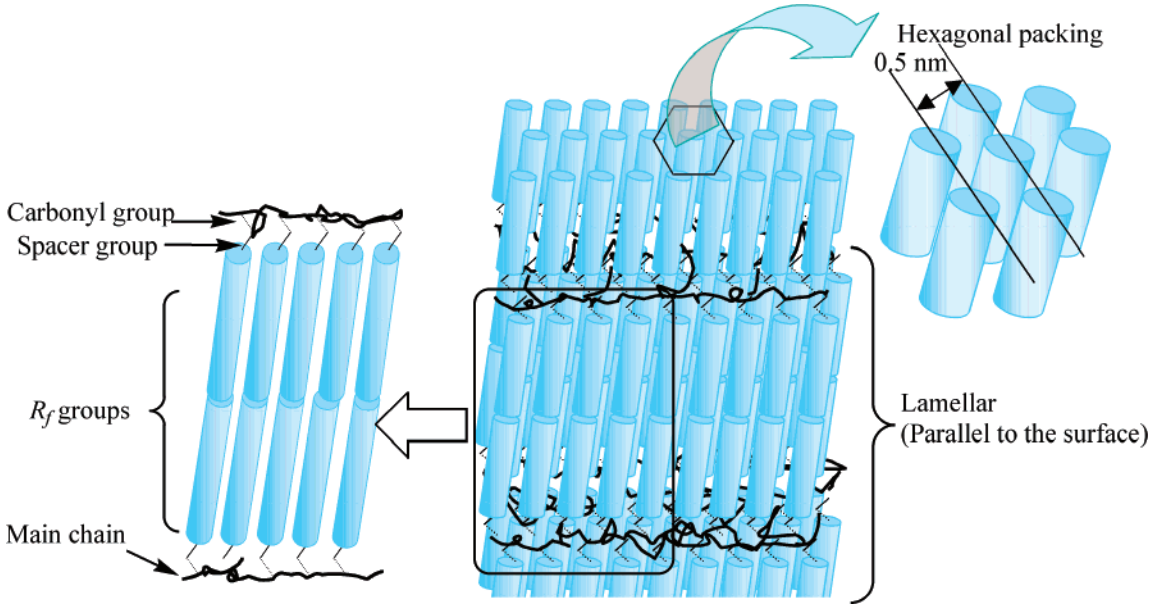

Figure 5. Schematic representation of molecular aggregation structure for the spin-coated PFA-C_y with $y \geq 8$ thin films.

is parallel to the substrate is obtained from bulk regions, indicating that the lamellar structure is oriented parallel to the substrate and that R_f groups are oriented almost perpendicular to the substrate, as shown in Figure 5.

On PFA-C_8, a comparison of the WAXD profiles before and after annealing [at 333 and 348 K (T_m) for 6 h] was also carried out. After annealing, peaks corresponding to the lamellar structure were sharpened. From these profiles, distortion of the crystal lattice was estimated on the basis of the paracrystalline theory proposed by Hosemann.[33−35] In the paracrystalline lattice model, the lattice vectors of adjacent unit cells vary in magnitude and direction due to large displacement of lattice points from their ideal positions, resulting in a loss of the long-range crystallographic order. On the assumption that the coordination statistics distribution function for the paracrystalline lattice model is in the form of a Gaussian distribution, the paracrystalline lattice factor $Z(s)$ of the hth-order reflection is defined as

$$Z(s) = Z(h) = [1 - \exp(-4\pi^2 g^2 h^2)]/ [(1 - \exp(-2\pi^2 g^2 h^2))^2 + (4 \sin^2 2\pi h) \exp((-2\pi^2 g^2 h^2)] \quad (2)$$

where s is the reciprocal lattice vector and g is the standard deviation of the Gaussian distribution divided by the average lattice vector $\tilde{a}$; the g is a parameter to evaluate the degree of paracrystalline disorder. The value of g is experimentally given by

$$(\delta\beta)^2 = (1/\tilde{a}^2)[(1/N^2) + \pi^4 g^4 h^4] \quad (3)$$

Here, $\delta\beta$ is the integral breadth of a reflection, h is the scattering order, and N is the number of scattering units. Figure 6a shows a plot of $(\delta\beta)^2$ as a function of h^4 for the (001), (002), and (003) reflections of PFA-C_8 and C_{10} thin films. A linear relation was obtained between the $(\delta\beta)^2$ and h^4 by the least-squares fitting method. The g and N were calculated using eq 2. Figure 6b shows the annealing temperature dependence of g and N for PFA-C_8 and C_{10} thin films. The g decreased from 6.1 × 10^{-2} to 2.6 × 10^{-2}, and N increased from ca. 7 to 24 as increasing annealing temperature. It therefore appears

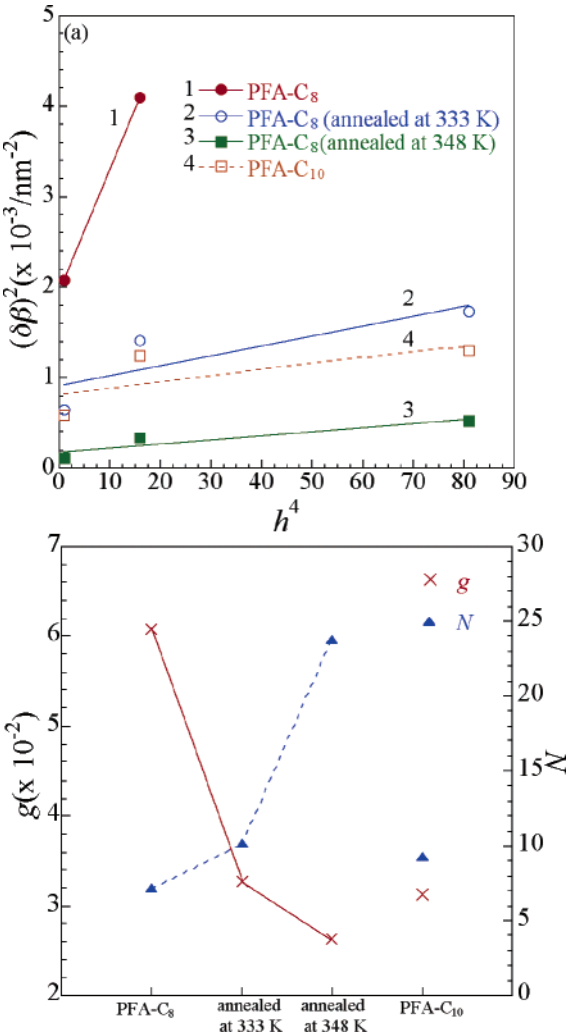

Figure 6. (a) Plot of $(\delta\beta)^2$ as a function of h^4 for the (001), (002), and (003) reflections of PFA-C_8 and PFA-C_{10} thin films and (b) the annealing temperature dependence of g and N for PFA-C_8 and PFA-C_{10} thin films.

that the paracrystalline distortion was decreased and that both the orientation and the order of the R_f groups were improved by annealing. PFA-C_{10} appears to have

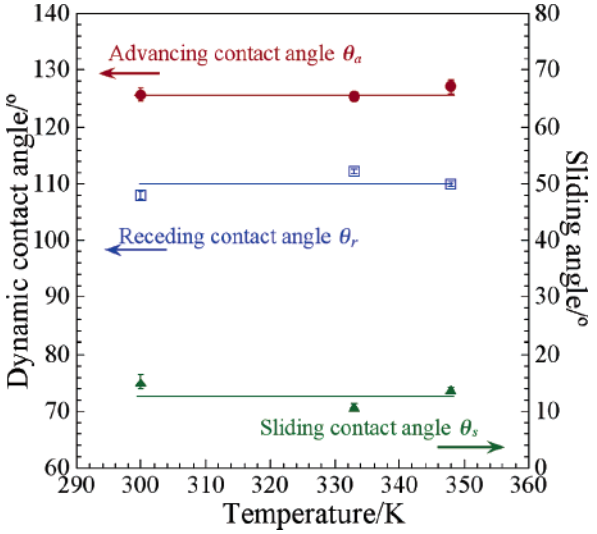

Figure 7. Effect of the annealing temperature on dynamic contact angle for spin-coated PFA-C_8 thin films against water (an inclinable plane, the droplet volume is 50 μL, T = 292 K).

a sufficiently high order of R_f groups, even without annealing.

In addition, the effects of annealing on the dynamic contact angle for spin-coated PFA-C_8 thin films against water were measured. Figure 7 shows the dynamic contact angle for spin-coated PFA-C_8 thin films against water (using an inclinable plane, the droplet volume is 50 μL, T = 292 K) after annealing at various temperatures. The small difference in the dynamic contact angle before and after annealing indicates that the ordering of R_f groups before annealing is sufficiently high for achieving high water repellency.

Surface Reorganization. On the basis of the above results, the following water repellent mechanism of PFA-C_y is proposed. In the case of PFA-C_y with $y \geq 8$, the mobility of the molecular chains is low because of the crystallization of R_f groups; therefore, lowering of the contact angle against water by reorientation of the R_f groups is very difficult. The change in the chemical composition in the surface area is indicative of the surface reorganization, owing to the reorientation of the R_f chains and exposure of the carbonyl groups in this case. To evaluate the surface reorganization behavior, X-ray photoelectron spectroscopic measurements in both dried and hydrated states as well as water contact angle measurements in water were carried out.

Figure 8 shows XPS C_{1s} spectra of (a) PFA-C_4 and (b) C_8 thin films in both dried and hydrated states. For the PFA-C_8 thin film, there was only a slight difference between the spectra. The intensities of CF_2 and CF_3 peaks, however, decreased drastically in the hydrated state in comparison with the dried state for PFA-C_4 films. Moreover, Figure 9 shows the results of F_{1s}/C_{1s} and O_{1s}/C_{1s} values of spin-coated PFA-C_y thin films in the dried and hydrated states, and the models for the water repellency of PFA-C_y thin films on the basis of the results of this study are presented in Figure 10. F_{1s}/C_{1s} and O_{1s}/C_{1s} values represent the relative magnitude of fluorine and oxygen concentrations at the surface. In the dried state, the F_{1s}/C_{1s} and O_{1s}/C_{1s} values completely agreed with the theoretical values, which are calculated from chemical structure of PFA-C_y. In the hydrated state, the F_{1s}/C_{1s} and O_{1s}/C_{1s} values did not change for PFA-C_y with $y \geq 8$; the F_{1s}/C_{1s} value, however, decreased, and the O_{1s}/C_{1s} value increased for PFA-C_y with

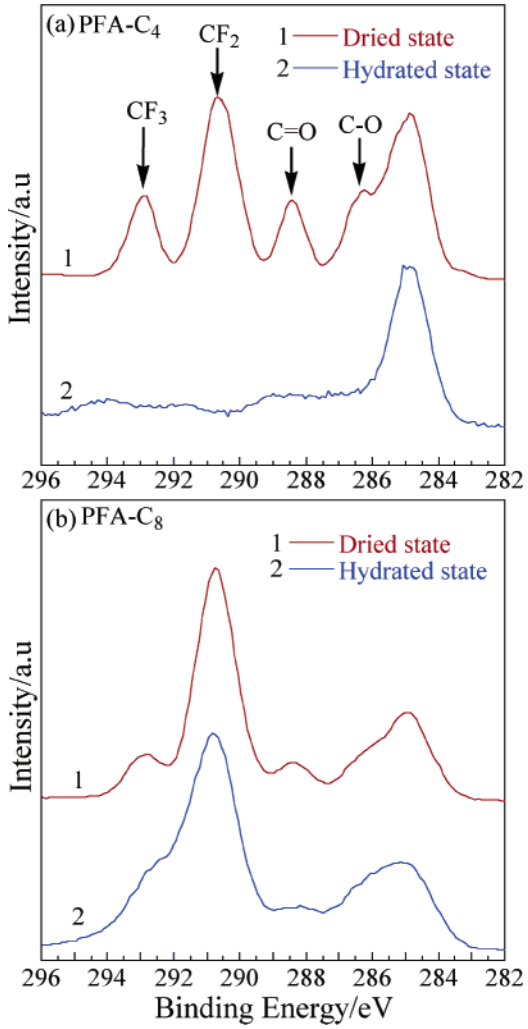

Figure 8. XPS C_{1s} spectra of (a) PFA-C_4 and (b) PFA-C_8 in the dried and hydrated state. In the hydrated state, the sample was hydrated by immersing in the water (T = 300 K) for 120 min and dried under vacuum (60 Pa) for 120 min. Takeoff angles are kept constant at 45°.

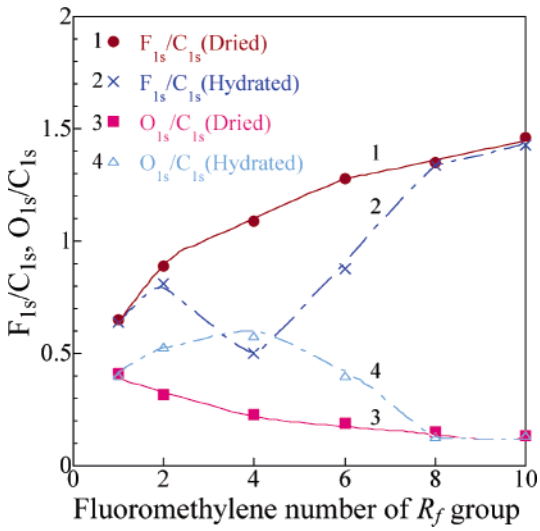

Figure 9. Dependence of F_{1s}/C_{1s} and O_{1s}/C_{1s} values in XPS spectra on the fluoromethylene number of the R_f groups in the dried and hydrated states.

$y \leq 6$. Low values of F_{1s}/C_{1s} and high values of O_{1s}/C_{1s} for PFA-C_y with $y \leq 6$ are probably derived from the reorientation of R_f groups and the exposure of carbonyl

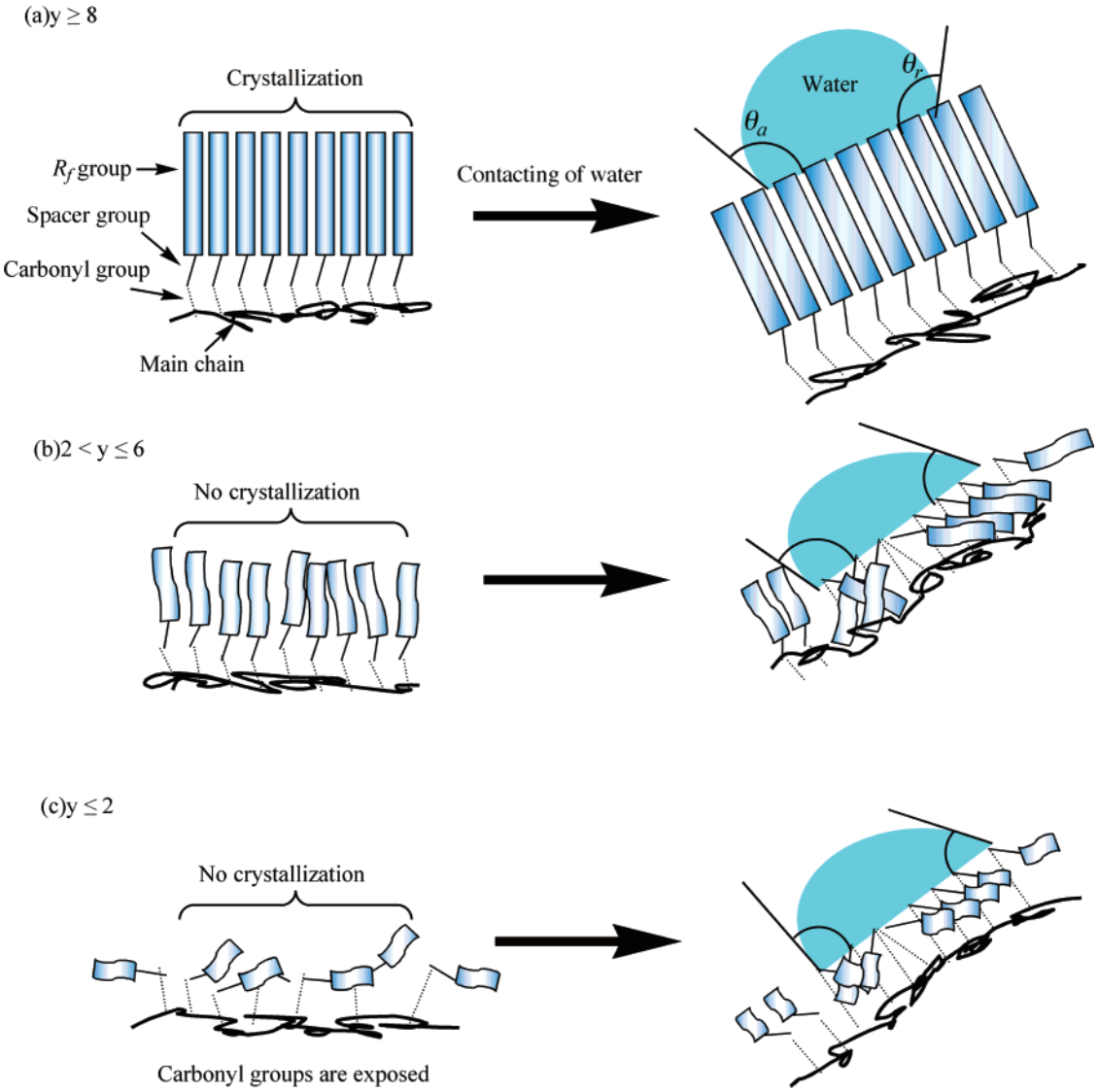

Figure 10. Models for water repellency of (a) PFA-C_y thin films with $y \geq 8$, (b) $2 < y \leq 6$, and (c) $y \leq 2$.

groups to the water interface (Figure 10b), and the constant values for PFA-C_y with $y \geq 8$ are derived from the inhibition of reorientation due to crystallization of the R_f groups (Figure 10a). It is likely that this reorientation of R_f chains with $y \leq 6$ at the surface is the greatest contributory factor to the observed decreased in the receding contact angle. In the case of PFA-C_1 and C_2, F_{1s}/C_{1s} and O_{1s}/C_{1s} values hardly changed, indicating that the molecular reorientation hardly occurred; however, the receding contact angles were very low. This is because the carbonyl groups have already been exposed to the air surface in the dried state, as the R_f groups are shorter than the others (Figure 10c). A similar result with regard to surface reorientation was also obtained for the contact angle measurement in water.

Figure 11 shows the dependence of the static contact angle in water on the fluoromethylene number of the R_f groups. The contact angle of water was small for PFA-C_y with $y \leq 6$ and increased drastically for PFA-C_y with $y \geq 8$, whereas the contact angle of methylene iodide was large for PFA-C_y with $y \leq 6$ and decreased for PFA-C_y with $y \geq 8$. Since it has been known that the contact angles of oil decreased on the surface with low surface free energy in water,[18] the obtained result indicates that a low surface free energy is maintained for PFA-C_y with $y \geq 8$. Actually, the surface free energy in water was calculated, and it showed a large value for PFA-C_y with $y \leq 6$ and decreased drastically for PFA-C_y with $y \geq 8$. Hence, these results also support the mechanism of a lowering receding contact angle for water by means of a reorientation of the R_f chains.

Conclusion

The relationship between surface properties and the fluoromethylene chain length of the R_f groups of PFA-C_y was investigated. PFA-C_y with $y \geq 8$ showed high dynamic water repellency. From DSC and WAXD measurements, it was clarified that PFA-C_y with $y \geq 8$ was in the crystalline state and formed ordered structures at the surface as well as in the bulk; the mobility of the molecular chains was therefore low. These results suggest that the water repellent mechanism of PFA-C_y could be attributed to the presence of highly ordered R_f chains with low mobility at the surface. XPS in dried and hydrated states and contact angle measurements in water showed that a reduced contact angle was caused by reorientation of the R_f chains and exposure of the carbonyl groups; these findings also supported a mechanism of lowering the contact angle of water by means of reorientation of the R_f chains with $y \leq 6$. Control of the mobility of the molecular chain seems to

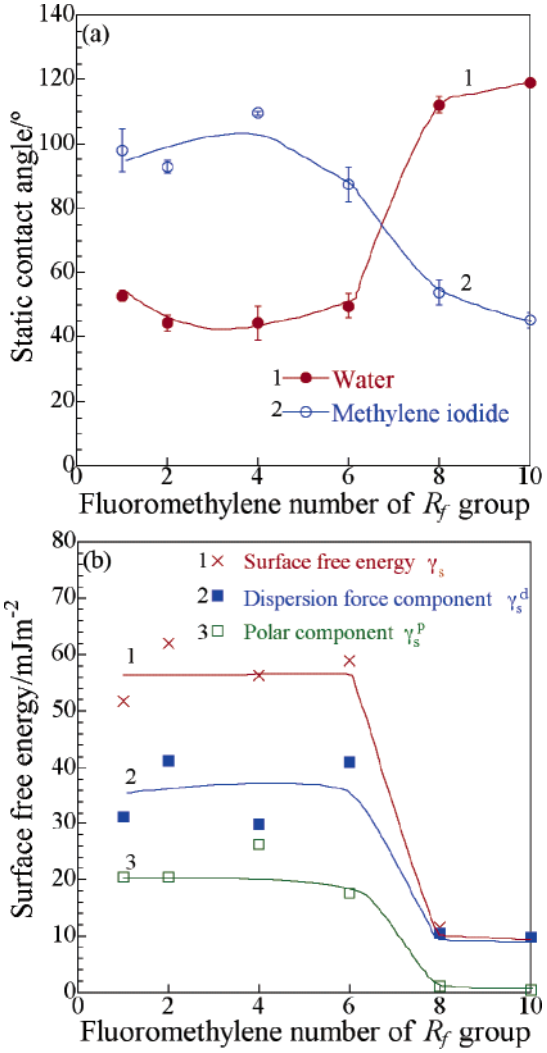

Figure 11. Dependence of (a) static contact angles against water and methylene iodide and (b) surface free energy in water (T = 300 K) on the fluoromethylene number of the R_f groups.

be one of the guidelines for the preparation of new R_f compounds with high water repellency.

Acknowledgment. This research was supported in part by a Grant-in-Aid for "Nanotechnology Researchers Network Center of Japan" (Kyushu University H15-028) and a Grant-in-Aid for the 21st century COE Program "Functional Innovation of Molecular Informatics" from the Ministry of Education Culture, Science, Sports and Technology of Japan. All samples provided by Daikin Industries Co., Ltd., was gratefully acknowledged.

References and Notes

(1) Pittman, A. G. In *Fluoropolymers*; Wall, L. A., Eds.; Wiley-Interscience: New York, 1972; p 419.
(2) Schmidt, D. L.; Coburn, C. E.; Dekoven, B. M.; Potter, G. E.; Meyers, G. F.; Fischer, D. A. *Nature (London)* **1994**, *368*, 39.
(3) Bernent, M. K.; Zisman, W. A. *J. Phys. Chem.* **1962**, *66*, 1207.
(4) Katano, Y.; Tomono, H.; Nakajima, T. *Macromolecules* **1994**, *27*, 2342.
(5) Morita, M.; Ogisu, H.; Kubo, M. *J. Appl. Polym. Sci.* **1999**, *73*, 1741.
(6) Sharfrin, E. G.; Zisman, W. A. *J. Phys. Chem.* **1960**, *64*, 519.
(7) Pittman, A. G.; Ludwig, B. A. *J. Polym. Sci., Part A1* **1969**, *7*, 3053.
(8) Ratner, B. D.; Weathersby, P. K.; Hoffman, A. S.; Kelly, M. A.; Scharpen, L. H. *J. Appl. Polym. Sci.* **1978**, *22*, 643.
(9) Andrade, J. D.; Gregoins, D. E.; Smith, L. M. In *Surface and Interfacial Aspects Chemistry and Polymers*; Andrade, J. D., Ed.; Plenum Press: New York, 1985; p 15.
(10) Damme, H. S. V.; Hogt, A. H.; Feijen, J. *J. Colloid Interface Sci.* **1986**, *114*, 167.
(11) Takahara, A.; Jo, N. J.; Kajiyama, T. *J. Biomater. Sci., Polym. Ed.* **1989**, *1*, 17.
(12) Takahara, A.; Jo, M. J.; Takamori, K.; Kajiyama, T. In *Progress in Biomedical Polymers*; Dunn, R. D., Gebelein, C. G., Eds.; Plenum Press: New York, 1990; p 217.
(13) Senshu, K.; Kobayashi, M.; Ikawa, N.; Yamashita, S.; Hirao, A.; Nakahama, S. *Langmuir* **1999**, *15*, 1763.
(14) Maekawa, T.; Kamata, S.; Matsuo, M. *J. Fluorine Chem.* **1991**, *54*, 84.
(15) Shimizu, T. In *Modern Fluoropolymers*; Scheirs, J., Ed.; John Wiley & Sons: New York, 1997; p 507.
(16) Owens, D. K.; Wendt, R. C. *J. Appl. Polym. Sci.* **1969**, *13*, 1741.
(17) Extrand, C. W.; Kumagai, Y. *J. Colloid Interface Sci.* **1997**, *191*, 378.
(18) Hamilton, W. C. *J. Colloid Interface Sci.* **1972**, *40*, 219.
(19) Nakamae, K.; Miyata, T.; Ootsuki, N. *Makromol. Chem., Rapid Commun.* **1993**, *14*, 413.
(20) Bongiovanni, R.; Maluceili, G.; Priola, A. *J. Colloid Interface Sci.* **1995**, *171*, 283.
(21) Johnson, R. E.; Dettre, R. H. *Surf. Colloid Sci.* **1969**, *2*, 85.
(22) Furmidge, C. G. L. *J. Colloid Sci.* **1962**, *17*, 309.
(23) Miwa, M.; Nakajima, A.; Fujishima, A.; Hashimoto, K.; Watanabe, T. *Langmuir* **2000**, *16*, 5754.
(24) Oner, D.; McCarthy, T. J. *Langmuir* **2000**, *16*, 7777.
(25) Morita, M.; Koga, T.; Otsuka, H.; Takahara, A. *Langmuir* **2005**, *21*, 911.
(26) McGrum, N. G.; Read, B. E.; Williams, G. In *Anelastic and Dielectric Effects in Polymeric Solids*; McGrum, N. G., Ed.; John Wiley & Sons: New York, 1967; p 238.
(27) Rogers, S. S.; Mandelkern, L. *J. Phys. Chem.* **1957**, *61*, 985.
(28) Takahara, A.; Morotomi, N.; Hiraoka, S.; Higashi, N.; Kunitake, T.; Kajiyama, T. *Macromolecules* **1989**, *22*, 617.
(29) Volkov, V. V.; Plate, N. A.; Takahara, A.; Kajiyama, T.; Amaya, N.; Murata, Y. *Polymer* **1992**, *33*, 1316.
(30) Volkov, V. V.; Fadeev, A. G.; Plate, N. A.; Amaya, N.; Murata, Y.; Takahara, A.; Kajiyama, T. *Polym. Bull. (Berlin)* **1994**, *32*, 193.
(31) Bunn, C. W.; Howells, E. R. *Nature (London)* **1954**, *174*, 549.
(32) Corpart, J. M.; Girault, S.; Juhué, D. *Langmuir* **2001**, *17*, 7237.
(33) Hosemann, R. *Z. Phys.* **1950**, *128*, 1−35, 42.
(34) Lindenmeyer, P. H.; Hosemann, R. *J. Appl. Phys.* **1963**, *34*, 42.
(35) Hosemann, R.; Hindeleh, A. M. *J. Macromol. Sci., Phys.* **1995**, *B34*, 327.

MA050394K